*Journal of Applied Fluid Mechanics*, Vol. 7, No. 1, pp. 103-110, 2014.
Available online at www.jafmonline.net, ISSN 1735-3572, EISSN 1735-3645.

# Pulsatile Flow in a Tapered U-Tube

M. Sumida

*Faculty of Engineering, Kinki University, Higashi-Hiroshima, Hiroshima, 739-2116 Japan*

Email: *sumida@hiro.kindai.ac.jp*

(Received November 11, 2012; accepted January 23, 2013)

**ABSTRACT**

An experimental investigation of pulsatile flow through a tapered 180° curved tube, i.e., a U-tube, was performed to study the blood flow in the aorta. The experiments were carried out in a U-tube with a curvature radius ratio of 3.5 and a 50% reduction in the cross-sectional area from the entrance to the exit of the curved section. Velocity measurements were conducted by a laser Doppler velocimetry (LDV) for a Womersley number of 10, a mean Dean number of 400 and a flow rate ratio of 1. Additionally, flow was visualized to qualitatively investigate the nature of the flow, complementing the quantitative LDV measurements. The velocity profiles for steady and pulsatile flows in the tapered U-tube were compared with the corresponding results in a U-tube having a uniform cross-sectional area. The striking effects of the tapering on the flow are exhibited in the axial velocity profiles in the section from the latter half of the bend to the downstream tangent immediately behind the bend exit. A depression in the velocity profile appears at a smaller turn angle $\Omega$ in the case of tapering, although the magnitude of the depression relative to the cross-sectional average velocity decreases. Near the bend exit, strong secondary-flow motion occurs, leading to a weak depression in the velocity profile in the downstream tangent immediately behind the bend exit. The value of $\beta$, which indicates the uniformity in the velocity profile over the cross section, decreases with increasing $\Omega$, whereas it rapidly increases immediately behind the bend exit.

**Keywords**: Experimental investigation, Unsteady flow, Curved tube, Tapering effect, Aortic arch, Velocity profile.

## 1. INTRODUCTION

In this paper, an experimental study on the velocity field of the pulsatile flow through a human aortic arch model is presented. The nature of the flow in the human arterial system has close relevance to the features of pulsatile flow in a curved tube. Therefore, unsteady flows in curved tubes have attracted the attention of many researchers, and steady progress is being made in this field. The arterial flow has been examined under various conditions using simplified models of both the physiological flow and blood vessels in an attempt to elucidate the complex flow phenomena in the living body. The aorta is a complex elastic curved tube with a nonplanar branch. Furthermore, blood with a non-Newtonian property flows intermittently and/or unsteadily. Among the models used in current research on blood flow in arteries, physiologists have recently become interested in the aortic arch model for the blood vessels and in the pulsatile and/or the physiological flows of periodically varying flow rate.

On the other hand, researchers in fluid engineering have also studied such unsteady flows in curved tubes from an industrial viewpoint. That is, they (for example, Walker *et al.*, 1989; Naruse *et al.*, 1990; Black *et al.*, 1995) performed the first studies of pulsatile flows through a U-tube. The U-tube employed in these studies had a curved part of 180°. Furthermore, the shape of the cross section was constant throughout the curved section. Taking into account these circumstances, the author (Sumida 2005, 2007) has grappled with the problem of pulsatile flows in curved tubes. He clarified that the flow phenomena in the entrance region of a curved tube are the most complicated for the moderate Womersley number.

On the basis of the achievements so far, it is desirable to develop a model of the flow in large arteries. In particular, the flow in the aortic arch has become a matter of great concern for many physiologists. Therefore, a study on the pulsatile flow in curved tubes with branching and tapering (Chandran, 1993) is also fervently hoped for. However, there have been very few studies (Yearwood and Chandran, 1980, 1984; Chandran and Ray, 1982) on flow in tapered curved tubes. Yearwood and Chandran (1980, 1984) conducted experiments on physiologically relevant pulsatile flow in a model of the human aortic arch. Furthermore, Chandran and Ray (1982) numerically examined the deformation of the tube wall for a tapering elastic curved tube with a reduction in cross-sectional area of 23%. However, unsteady flows through tapered curved tubes, into which a fully developed straight-tube flow enters, have not been treated to the best of the author's knowledge. Therefore, it is necessary to investigate

such flows to elucidate the flow mechanism in the aortic arch.

Flow in the human aorta is mainly determined by two nondimensional parameters: the Womersley number $\alpha$ and the Reynolds number *Re*. Here, $\alpha$ is defined as $d_1(\omega/\nu)^{1/2}/2$ and *Re* as $d_1W_1/\nu$, in which $\nu$ is the kinematic viscosity of the fluid and *W* is the instantaneous cross-sectional average velocity, the subscript 1 indicating the upstream tube. Please refer to Fig. 2, which will be presented later, for the symbols. With regard to the parameters, a wide range of values, namely, $\alpha$ of 8 to 21 and *Re* of 1000 to 8000, are well known to correspond to flow in the human aorta (Okino *et al.*, 1986; Ohshima, 1995). Furthermore, a typical aortic arch for real situation ranges in tapering from 50 to 60% and in a curvature radius ratio *Rc* from 3 to 4 (Okino *et al.*, 1986), in which *Rc* is the ratio of the curvature radius *R* of the tube axis to the tube radius $d_1/2$.

In this study, we examined the effect of only the tapering on the flow in the human aortic arch. To do this, we carried out measurements of flows in a planar U-tube with a tapering of 50% in cross-sectional area from the entrance to the exit and with a curvature radius ratio *Rc* of 3.5. That is, we first obtained a general view of the velocity profiles of the axial flow by the hydrogen bubble method for Womersley numbers $\alpha$ ranging from 5.5 to 18. Subsequently, LDV measurements of the velocity profiles were performed for a moderate Womersley number flow. In addition, the secondary-flow motion induced in the cross section was also visualized and photographed. Finally, comparing these results with those obtained for a U-tube with a constant cross-sectional area, we clarified the effects of tapering on the pulsatile flow characteristics.

## 2. Experimental Apparatus and Procedures

### 2.1 Experimental Apparatus

A schematic diagram of the experimental apparatus is shown in Fig. 1. The system consists of a pulsatile flow generator, a tapered U-tube used as a model of the aortic arch and velocity-measuring and visualization devices. The working fluid was water at a temperature of 20°C. This experimental system is almost the same as that employed by Sumida (2005, 2007) for measurements of the pulsatile entrance flow in curved pipes and U-tubes. A sinusoidal pulsatile flow was obtained by superimposing a volume-cycled oscillatory flow on a steady flow. The oscillatory flow was generated by a reciprocating piston pump installed in a scotch yoke mechanism. The steady flow component was supplied by a magnetic pump. Thus, the desired pulsatile flow rate was effectuated in the test U-tube, and the periodically varying flow rate Q is expressed as

$$Q = Q_m + Q_o \sin\Theta, \tag{1}$$

where $\Theta$ ($=\omega t$) is the phase angle, $\omega$ is the angular frequency of pulsation and *t* is time. Moreover, the subscripts *m* and *o* indicate mean over time and amplitude, respectively.

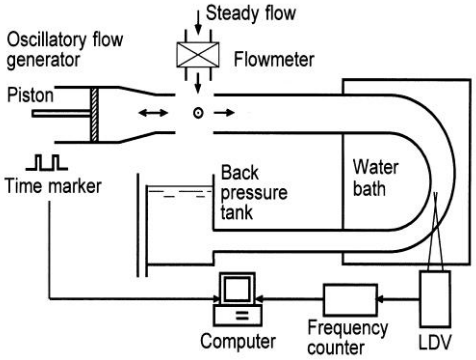


**Fig. 1.** Schematic diagram of experimental apparatus.

### 2.2 Test U-tube as an Aortic Arch Model

Figure 2 shows the aortic arch model together with the coordinate system, in which $\Omega$ is the turn angle measured along the tube axis from the entrance of the bend. The tapered U-tube was made of a transparent glass tube. The dimensions were based on models employed in previous works (Walker *et al.*, 1989; Naruse *et al.*, 1990; Black *et al.*, 1995; Yearwood and Chandran, 1980, 1984; Chandran and Ray, 1982; Kang and Tarbell, 1983; Lim *et al.*, 1984) on aortic arch flows and also based on books (Okino *et al.*, 1986; Ohshima, 1995) on the blood circulatory system. That is, the test U-tube had inside diameters of $d_1$=23.1 mm and $d_2$=16.3 mm, respectively, at the entrance and exit of the curved section with a curvature radius of *R*=40 mm. This gives a reduction ratio of 50% in the cross-sectional area from the entrance to the exit. Furthermore, these values correspond to a curvature radius ratio of $Rc=R/(d_1/2)=3.5$.

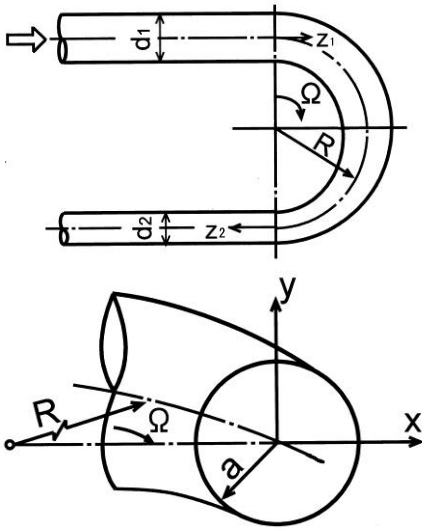


**Fig. 2.** Configuration of tapered U-tube (upper figure) and coordinate system (lower figure).

A U-tube having a constant cross-sectional area was also employed in the present experiment for comparison. Its inside diameter was *d* (=2*a*)=17.6 mm and the curvature radius was *R*=32 mm, corresponding

to $Rc$ (=$R/a$)=3.6, similar to that of the tapered U-tube. Both ends of the bend of each U-tube were attached to long straight tubes. The lengths of the upstream and downstream tubes were about 2000 and 1800 mm, respectively. This ensures that a fully developed straight-tube pulsatile flow enters the curved section.

### 2.3 Velocity Measurements and Visualization Method

The velocity measurements were performed with a LDV system (Kanomax, System 8832) using a 3W argon laser in the backscattering mode. The output of the frequency counter was recorded synchronously with a time marker signal indicating the position of the piston and was converted to velocity data using a personal computer. Furthermore, the phase-averaged velocity was obtained from the data of about 10–20 cycles. A detailed description of the above data acquisition method for a pulsatile flow can be found in a previous work of the author (Sumida, 2007). The measurements were executed at 15 streamwise stations between $z_1$=–7$d_1$ in the upstream tube and $z_2$=30$d_2$ in the downstream tube. Axial flow velocity $w$ and outward secondary-flow velocity $u$ were obtained at each station. Concretely, the axial velocity $w$ was measured at 72 grid points in the upper half of the cross section, while the outward velocity $u$ was measured on the $x$- and $y$-axes. Measurement errors of velocity were estimated to be less than 4% except near the tube wall, which is described in detail in the earlier work (Sumida, 2007).

Before executing the LDV measurements, visualization experiments were carried out to observe flows throughout both U-tubes. The axial flow was rendered visible by the hydrogen bubble method. On the other hand, the secondary-flow motion induced in the cross section of the curved part of the U-tubes was also visualized by the solid tracer method (Sumida *et al.*, 1989, and Sudo *et al.*, 1992).

## 3. Results and Discussion

### 3.1 Pulsatile Flow Condition

In this study, the experiments were carried out under the conditions of a mean Reynolds number $Re_m$ of 748, Womersley numbers $\alpha$ of 5.5 to 18 and a flow rate ratio $\eta$ of 1. Here, $\eta$ is expressed as $\eta$=$W_o/W_m$ (=$Q_o/Q_m$). A Dean number $D$ is defined as $D$=$ReRc^{-1/2}$, and a mean Dean number $D_m$ in this study was 400. These values were chosen with reference to previous works (Walker *et al.*, 1989; Naruse *et al.*, 1990; Black *et al.*, 1995; Yearwood and Chandran, 1980, 1984; Kang and Tarbell 1983; Lim *et al.*, 1984; Sumida *et al.*, 1989; Sumida and Sudo, 1986) on modeled aortic arch flows and/or pulsatile flows in curved tubes.

In the following, we will focus on the results for a moderate $\alpha$ of 10. For the pulsatile entrance flow in curved tubes without tapering, peculiar, complicated velocity profiles appear under this flow condition (Sumida, 2005, 2007). By comparing results for the tapered U-tube with those for the nontapered U-tube, we discuss and clarify the effects of tapering on pulsatile flow in a U-tube.

### 3.2 Steady Flow

There are two experimental works on steady flow through a tapered U-tube: Yearwood and Chandran (1980) and Kang and Tarbell (1983). Kang and Tarbell (1983) measured the pressure drop between the entrance and exit of the curved section. Yearwood and Chandran (1980) performed hot-film anemometry measurements for an aortic arch model with nonplanar curvature to obtain velocity profiles. However, for a planar U-tube with tapering, there have been no studies, even on steady flow. Therefore, we examined the steady flow before investigating the pulsatile flow. In the present paper, nevertheless, the illustration is omitted.

### 3.3 Pulsatile Flow

#### *3.3.1 Changes in Velocity Profiles along the Tube Axis*

The axial velocity profiles on the $x$- and $y$-axes are shown in Fig. 3. In the figure, the velocities are normalized by the maximum value of the cross-sectional average velocity, $W_{1,m}$+ $W_{1,o}$, in the upstream tube. The profiles are illustrated for four representative phases in a pulsation cycle. For comparison, the results for the nontapered U-tube are also presented in Fig. 4 for the phases with the maximum and minimum flow rates ($\Theta$=90, 270°). Moreover, the profiles of the secondary flow velocity on the $x$-axis in the tapered and nontapered U-tubes are given in Figs. 5 and 6, respectively.

In a pulsatile flow in curved tubes, there occur the phenomena of flow reversal near the inner wall and the depression in the axial velocity profile at the middle of the accelerative phase ($\Theta$≈0°) (Sumida and Sudo, 1986; Sumida *et al.*, 1989; Sumida, 2007). Moreover, the velocity profiles behind the bend entrance exhibit very complicated changes near the inner region at certain $\Omega$ and $\Theta$. In particular, for the tapered U-tube, in which the cross-sectional average velocity increases with $\Omega$, these phenomena and characteristics become combined in a complicated manner in a short section. Consequently, the pulsatile flow exhibits complex velocity profiles that change with time. Below, on the basis of such a general view of the flow characteristics, we discuss and extract the effect of tapering on the pulsatile flow in comparison with that for a nontapered U-tube.

Near the beginning of the bend, the effect of curvature on the flow is evident, whereas the effect of tapering is rather small. That is, at the section with $z_1/d_1$=–3 in the upstream straight tube, there is no apparent effect of the downstream bending in the flow. However, immediately behind the bend entrance ($\Omega$≈0–10°), the fluid in the inner part of the cross section is forced downwards by the large axial pressure gradient occurring on the inner wall in the latter half of the accelerative phase. For the phase with the large flow rate starting from the end of the accelerative phase ($\Theta$≈90–150°), the region with higher axial velocity temporarily becomes biased further to the inner wall compared with that for the nontapered U-tube. Simultaneously, the fluid with higher speed is subjected to a strong centrifugal force. As a result, slightly

downstream, at $\Omega$=20°, the secondary-flow velocity rapidly increases in the first half of the decelerative phase ($\Theta$=90–180°) and is larger than that for the nontapered U-tube as shown in Fig. 4. On the other hand, the shift of the higher-axial-velocity region toward the outer wall causes the axial momentum in the inner part of the cross section to further reduce in the latter half of the decelerative phase ($\Theta$=180–270°). Therefore, the region where the fluid flows in the negative direction at the minimum flow rate ($\Theta$=270°) extends further toward the outer wall in comparison with that for the nontapered U-tube ($\Omega$=20°).

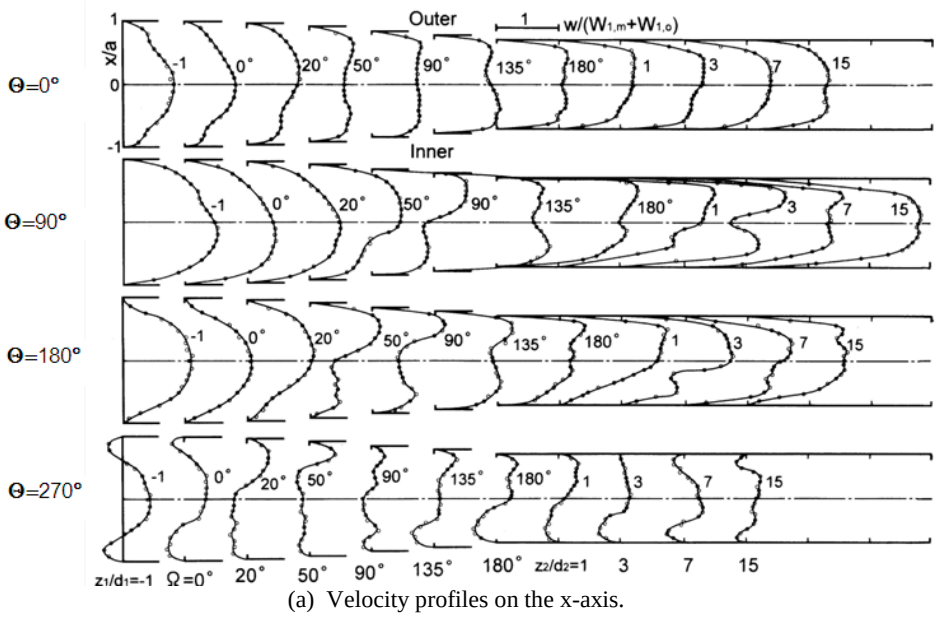


(a) Velocity profiles on the x-axis.

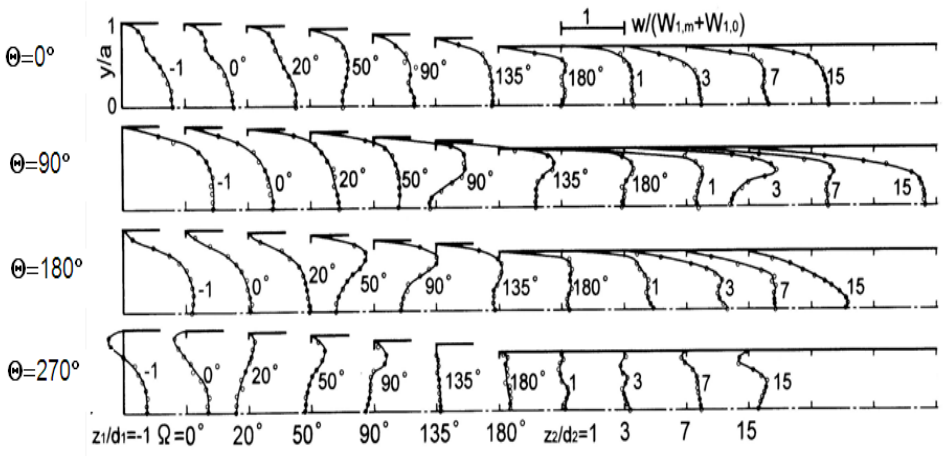


(b) Velocity profiles on the *y*-axis.

**Fig. 3.** Axial velocity profiles of pulsatile flow through tapered U-tube ($\alpha$=10, $D_m$=400, $\eta$=1).

Nevertheless, in the section from $\Omega$=50 to 90°, the difference between the magnitudes of the positive and negative velocities decreases. Furthermore, for $\Omega$=50–90°, the flow in the first half of the decelerative phase ($\Theta$=90–200°) exhibits complicated profiles of its axial velocity. In this section, the secondary motion is biased to the inner part of the cross section as can be seen in the photograph in Fig. 7 for $\Omega$=50°. The secondary-flow velocity at $\Theta$=90° is about 40% larger than that for the nontapered U-tube as shown in Fig. 5 and Fig. 6 for $\Omega$=90°.

For a curved tube without tapering, the depression in the velocity profiles appears at the middle of the accelerative phase ($\Theta$≈0°) for a nearly fully developed flow with a moderate Womersley number, which was reported by Sumida and Sudo (1986), Sumida *et al.* (1989) and Sumida (2007). In particular, for strongly curved tubes (Sumida, 2005), this phenomenon also occurs at the location with a non-dimensionalized distance $Rc^{1/2}\Omega$ ($\Omega$: rad) of approximately 2 downstream of the entrance and in the first half of the decelerative phase ($\Theta$≈90–180°). The effect that strong secondary-flow motion has on the axial velocity profiles is very interesting. Moreover, the depression

profile in the axial velocity is formed at a smaller $\Omega$ than that for the nontapered U-tube. This is, as stated above, attributed to the additive effects of the secondary-flow conveyance and the axial acceleration near the inner wall. However, the magnitude of the depression relative to the instantaneous cross-sectional average velocity $W$ is less than that for the nontapered U-tube. This stems from the fact that the fluid in the inner part of the tube has been axially accelerated before the depression profile is formed.

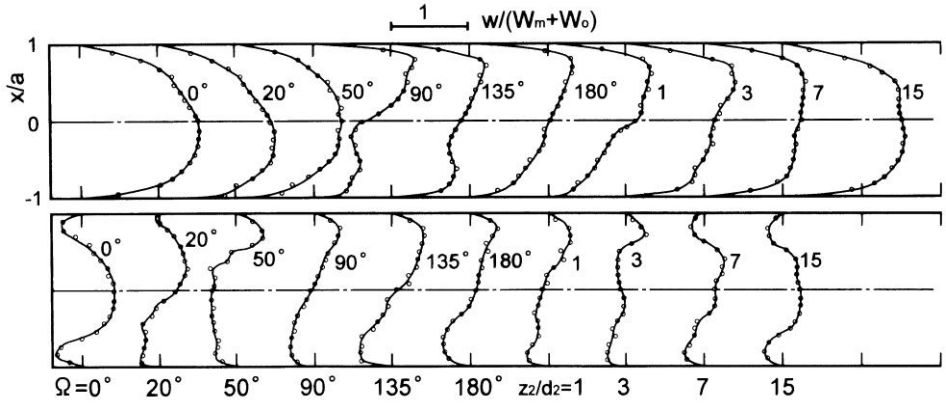


(a) Velocity profiles on the *x*-axis.

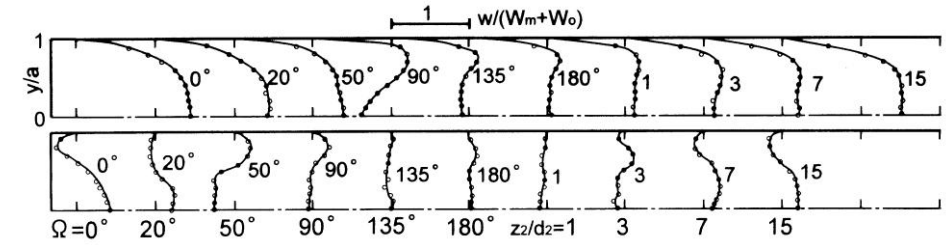


(b) Velocity profiles on the *y*-axis.

**Fig. 4.** Axial velocity profiles of pulsatile flow through nontapered U-tube ($\alpha$=10, $D_m$=400, $\eta$=1).

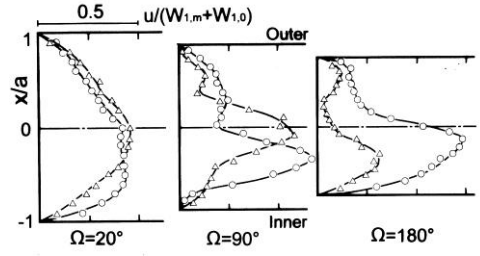


**Fig. 5.** Outward velocity profiles on the *x*-axis for pulsatile flow through tapered U-tube ($\alpha$=10, $D_m$=400, $\eta$=1). ○: $\Theta$=90°, Δ: $\Theta$=180°.

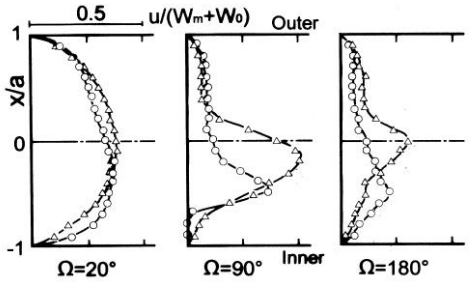


**Fig. 6.** Outward velocity profiles on the *x*-axis for pulsatile flow through nontapered U-tube ($\alpha$=10, $D_m$=400, $\eta$=1). ○: $\Theta$=90°, Δ: $\Theta$=180°.

Downstream from the middle of the tapered bend, in accordance with the increase in $W$, the unsteady inertia force acting on the fluid motion becomes strong. Simultaneously, the centrifugal force acting on the fluid increases and also the pressure difference between the inner and outer walls rises. As a result, the pressure drop along the tube axis on the inner wall further increases in the accelerative phase when the flow rate increases. Thus, in the latter half of the accelerative phase ($\Theta$=0–90°), the axial velocity takes a maximum near the inner wall ($\Omega$≈135°). Moreover, the differences in the amplitude and phase of the axial velocity variation in the cross section are reduced, although the variation of velocity becomes slightly larger in the inner part of the cross section. For the nontapered U-tube, the $w$ profile at $\Omega$=135° has a similar shape to that in a fully developed state in a curved tube (Sumida and Sudo, 1986), as shown in Fig. 4.

In the section closer to the bend exit, the pressure drop along the tube axis is reduced on the inner wall. The fluid flowing with a higher speed in the phase with a large flow rate in the inner region of the tube is pushed toward the outer wall. Thus, the fluid with strong secondary-flow motion streams out into the downstream straight tube, as shown in Fig. 5. In the downstream tube, no centrifugal force acts on the fluid.

Nevertheless, as the higher-speed fluid flows downward, the region with the maximum speed migrates in the cross section in a manner dependent on both $z_2$ and $\Theta$. This behavior for the tapered U-tube is considerably different from that for the nontapered U-tube. That is, the outward velocity $u$ of the secondary flow at the bend exit ($\Omega$=180°) is large in the inner part of the tube, with $u$ increasing in proportion to the flow rate as shown in Fig. 5. Its speed reaches as high as 60% of the instantaneous cross-sectional average velocity $W_{2,m}$ in the downstream straight tube. When we inspect the magnitude of the secondary-flow velocity relative to the axial-flow velocity, we can see that at the bend exit, the secondary-flow motion occurs with a similar strength to that immediately behind the bend entrance.

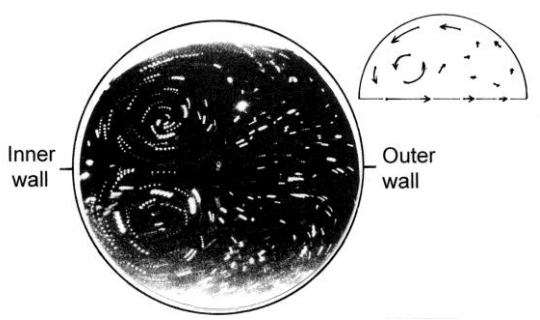


**Fig. 7.** Secondary-flow motion visualized by tracer method for pulsatile flow through tapered U-tube ($\alpha$ =10, $D_m$ = 400, $\eta$ =1). $\Omega$=50°, $\Theta$=180°.

Immediately behind the bend exit of the tapered U-tube, from $\Omega$=180° to $z_2/d_2$=1, owing to this strong secondary flow, the axial velocity is large along the side of the outer wall throughout the pulsation cycle. However, at $z_2/d_2$≈3, the flow takes a maximum axial velocity, even in the inner part of the tube, in the first half of the decelerative phase ($\Theta$=90–150°). This again leads to the $w$ profile being slightly lower in its central part. Moreover, at the bend exit ($\Omega$=180°), the region of backward flow again extends in the inner part of the cross section at the end of the decelerative phase ($\Theta$=270°). After that, the velocity profile is gradually changed, owing to the viscosity, symmetrically with respect to the tube axis ($z_2/d_2$=7–15). However, the recovery length of the flow in the downstream tube to a fully developed straight-tube flow with respect to $z_2/d_2$ is slightly longer than that for the nontapered U-tube. It appears that in the downstream tube, the flow involving the strong secondary-flow motion becomes a flow with a high Reynolds number [$Re_{2m}$ ($=W_{2m}d_2/\nu$)=1060] and low Womersley number {$\alpha_2$ [$=d_2(\omega/\nu)^{1/2}/2$)]≈7}.

### *3.3.2 Flattening the Profiles of Axial Flow Velocity*

As stated previously, in a pulsatile flow through the U-tube with tapering, the higher-speed region of the primary flow shifts alternately toward the outer and inner walls of the cross section with increasing turn angle. That is, it first migrates toward the outer part, then toward the inner part, and then toward the outer part of the cross section in the U-tube. Therefore, the axial velocity profile changes in a complicated manner with the phase $\Theta$ and also in the streamwise directions of $\Omega$ and $z_2$. It is well known that reducing the cross-sectional area along the tube axis generally has the effect of flattening the velocity profile. Thus, to evaluate the uniformity of the axial flow velocity, we introduce the following quantity.

$$\beta = \frac{1}{AW_m}\int_A |w - W|\, dA \tag{2}$$

Here, $A$ is the cross-sectional area of the tube. The values of $\beta$ for different $\Theta$ are given in Fig. 8. Additionally, Fig. 9 illustrates the axial changes in $\beta_m$, which is the time-averaged value of $\beta$, along the tube axis. In Figs. 8 and 9, the results for the nontapered U-tube and for a steady flow are also displayed for comparison.

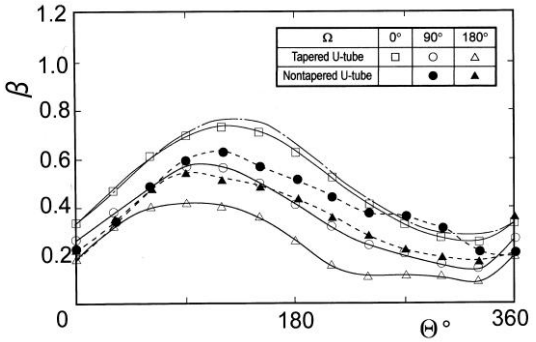


**Fig. 8.** Variation of uniformity $\beta$ of velocity profiles over a cycle. (——– – ——: Fully developed straight-tube flow)

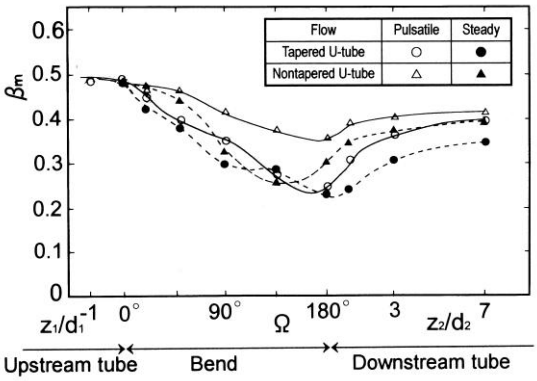


**Fig. 9.** Axial variation of time-averaged uniformity $\beta_m$ of velocity profiles.

In a fully developed straight-tube flow, both $\beta$ and $\beta_m$ for the steady and pulsatile flows, respectively, take a value of about 0.5. From Fig. 8, it can be seen that $\beta$ at the bend entrance varies sinusoidally with a phase lag of about 40°, although the flow has velocity profiles similar to those in the fully developed straight-tube flow. Also, the degree of the lag corresponds to the phase difference between the variations in velocity in the central part of the cross section and in the boundary layer on the tube wall. With increasing $\Omega$, however, $\beta$ decreases from the latter half of the decelerative phase to the first stage of the accelerative phase. This shows that the velocity profile is flattened. Furthermore, the time at which $\beta$ takes a maximum shifts to the phase of the maximum flow rate.

In the bend of the tapered U-tube, $\beta_m$ for the pulsatile flow is not significantly different from that in the steady flow as shown in Fig. 11. As $\Omega$ increases, $\beta_m$ decreases, and the velocity profile is flattened the most at the end of the bend. Immediately behind the bend exit, at $z_2/d_2$=0–3, $\beta_m$ rapidly increases to approximately take the value at $\Omega\approx$75° in the bend. This is due to the abrupt change in the velocity profile of the pulsatile flow. Downstream, $\beta_m$ gradually approaches 0.5 in the case of axisymmetric flow. For the non-tapered U-tube, on the other hand, $\beta_m$ for the pulsatile flow varies less with $\Omega$. This is because the higher-speed region is still in the outer part of the tube throughout the cycle. In the steady flow, $\beta_m$ decreases in the bend since the axial flow starts to exhibit velocity profiles having a maximum not only near the outer wall but also near the inner wall. Furthermore, $\beta_m$ in the latter half of the bend, where the depression phenomenon almost disappears, takes approximately the same value as that for the tapered U-tube ($\Omega\approx$135°).

## 4. CONCLUSION

An experimental investigation has been performed on pulsatile flow through a tapered U-tube having a curvature radius ratio of $Rc$=3.5, where the rate of reduction of the cross-sectional area from the entrance to the exit of the bend is 50%. The flow field was examined by LDV for $\alpha$=10, $D_m$=400 and $\eta$=1. The following findings were obtained from this study.

(1) The effects of tapering on both pulsatile and steady flows are marked in the section from the latter half of the bend to the vicinity of the exit of the bend. The flows exhibit characteristics significantly different from those for the nontapered U-tube.

(2) The peculiar phenomenon of the depression in the axial velocity profile, which occurs in the pulsatile entrance flow in curved tubes, appears at a smaller $\Omega$ than that for the U-tube without tapering. However, the degree of depression is smaller. Near the bend exit, the secondary-flow motion is abruptly intensified and a weak depression appears in the axial velocity profiles in the straight tube downstream from this point.

(3) For the pulsatile flow, as $\Omega$ increases, the velocity profiles change to a shape indicating a small difference in the value of speed in the cross section. Although $\beta_m$ is less than that for the U-tube without tapering, immediately behind the bend exit it increases rapidly.

## ACKNOWLEDGEMENT

This work was supported in part by MEXT-Supported Program for the Strategic Research Foundation at Private Universities (Grant No. S0901045).

## REFERENCES

Black, M. M., D.R., Hose, and P.V., Lawford (1995). The origin and significance of secondary flows in the aortic arch. *Journal of Medical Engineering & Technology*, 19 (6), 192-197.

Chandran, K. B. and G., Ray (1982). Clinical implications of pressure deformation analysis of curved elastic tubes. *Medical & Biological Engineering & Computing*, 20, 145-150.

Chandran, K. B. (1993). Flow dynamics in the human aorta. *Transactions of the ASME, Journal of Biomechanical Engineering*, 115, 611-616.

Kang, S. G. and J.M., Tarbell (1983). The impedance of curved artery models. *Transactions of the ASME, Journal of Biomechanical Engineering*, 105, 275-282.

Lim, K.O., J.S., Kennedy, and C.M., Rodkiewicz (1984). Entry flow in a circular tube of aortic arch dimensions. *Transactions of the ASME, Journal of Biomechanical Engineering*, 106, 351-356.

Naruse, T., Y., Nishina, S., Kugenuma, and K., Tanishita (1990). Developing pulsatile flow in the aortic arch. *Transactions of the JSME Ser B,* 56 (532), 3625-3632 (in Japanese).

Ohshima, N. (1995). Blood circulating system from the viewpoint of hydrodynamics. *Nagare*, 14 (1), 5-9 (in Japanese).

Okino, H., M., Sugawara, H., Matsuo (1986). Measurements and mechanics of cardiovascular system. *Kodansya*, Tokyo, 186 (in Japanese).

Sudo, K., M., Sumida, and R., Yamane (1992). Secondary motion of fully developed oscillatory flow in a curved pipe. *Journal of Fluid Mechanics*, 237, 189-208.

Sumida, M. (2005). Experimental investigation of pulsating laminar flow through U-tubes; Effect of various parameters. *Proceedings of the 8th International Symposium on Fluid Control, Measurement and Visualization*, Chengdu, China, Paper No. 12-4.

Sumida, M. (2007). Pulsatile entrance flow in curved pipes; Effect of various parameters. *Experiments in Fluids*, 43, 949-958.

Sumida, M. and K., Sudo (1986). Pulsating flow in curved pipes; 3rd report: Axial velocity profile. *Bulletin of JSME*, 29 (256), 3334-3340.

Sumida, M., K., Sudo, and H., Wada (1989). Pulsating flow in a curved pipe; Secondary flow. *JSME International Journal*, 32 (4), 523-531.

Walker, J. D., W.G., Tiederman, and W.M., Phillips (1989). Effect of tilting disk, heart valve orientation on flow through a curved aortic model. *Transactions of the ASME, Journal of Biomechanical Engineering*, 111, 228-232.

Yearwood, T. L. and K.B., Chandran (1980). Experimental investigation of steady flow through a model of the human aortic arch. *Journal of Biomechanics*, 13, 1075-1088.

Yearwood, T. L. and K.B., Chandran (1984). Physiological pulsatile flow experiments in a model of the human aortic arch. *Journal of Biomechanics*, 15 (9), 683-704.